Electrochimica Acta 117 (2014) 329–335

Contents lists available at ScienceDirect

Electrochimica Acta

journal homepage: www.elsevier.com/locate/electacta

Effect of electrolyte composition on TiO_2 nanotubular structure formation and its electrochemical evaluation

K.M. Deen[a], A. Farooq[a], M.A. Raza[a], W. Haider[b,*]

[a] Department of Metallurgy and Materials Engineering, CEET, University of the Punjab, 54590, Lahore, Pakistan
[b] Mechanical Engineering Department, The University of Texas Pan American, Edinburg, TX, 78539, US

ARTICLE INFO

Article history:
Received 9 September 2013
Received in revised form
18 November 2013
Accepted 20 November 2013
Available online 7 December 2013

Keywords:
Nanotubular
Electrochemical
Photocatalytic
Impedance Spectroscopy

ABSTRACT

Nanotubular structures of TiO2 were synthesized on Ti6Al4 V alloy in various electrolytes with and without fluoride ions and were then evaluated by potentiodynamic polarization tests and electrochemical impedance spectroscopy. The resultant surface features were revealed through scanning electron microscopy. It was observed that barrier type oxide film is formed in halide free acidic electrolyte. From potentiodynamic polarization scans it was deduced that high current density in 0.15 M NH_4F containing electrolyte corresponded to the formation of TiO_2 nanotubes by slow field driven Ti^{4+} ions diffusion in the electrolyte than field assisted TiO_2 growth. Two time constant impedance spectra were simulated to the field assisted charge transfer reactions at high frequency (dissolution of TiO_2 by fluoride ions) and at low frequency (adsorption of oxidase ions) regime. X-ray diffraction pattern of as anodized surface revealed oxygen deficient Ti_6O phase, which was converted to rutile/anatase phases by heat treatment in air.

1. Introduction

Titanium and its alloys are of great importance because of their excellent properties and efficient performance in widespread applications i.e. photo-catalysis, self-cleaning processes, solar cells, fuel cells, catalysis, gas sensing devices, semiconductors doping, biomedical, interference coatings, and manufacturing optical devices etc. The self-healing nature and compactness of passive film make it suitable for many hostile environments. It is also possible to intentionally grow titanium dioxide (TiO_2) passive film of varying thickness, morphologies and structure or may be tuned as per requirements [1,2].

Nanoporous or self-organized nanotubular TiO_2 structure on titanium surface can be produced by simple electrochemical anodization in fluoride containing electrolytes. The process parameters such as time, solution concentration, applied potential and potential ramp greatly influence the surface morphology, shape, dimensions and activity of the grown nanostructure [3]. The variation of process parameters during growth of nanotubular structure could also influence the crystal structure of TiO_2. Schultze et al., [4] reported that the crystalline TiO_2 is formed at higher voltage while amorphous TiO_2 is formed at relatively low voltage. Adjusting the potential and varying the composition of electrolyte can also vary the diameter of nanotubes. The length of nanotube could be controlled by varying pH of the electrolyte and/or by changing anodizing time. In other words, the morphology, structure, dimensions and pattern of nanotubes growth strongly depend on electrolyte composition, pH, applied potential and time [5].

Highly ordered, aligned TiO_2 nanotubes can be produced efficiently by electrochemical anodization process. The self-organized 65 nm diameter TiO_2 nanotubes in 0.5-3.5% HF solutions was produced by D. Gong et al. and it was concluded that anodization time did not affect the length of nanotubes (NTs) [6]. π-TiO_2 self-organized nanotubes of 500 nm long were prepared by A. Ghicov et al. in PO_4^{2-}/F^- solutions. In fluoride containing electrolytes with addition of $NH_4H_2PO_4$ it was possible to produce 4 mm long and 100 nm diameter nanotubes. This study also investigated the inverse relation between nanotubes wall thickness and pH of electrolyte [7]. In another study, Bauer et al. [8] optimized the concentration of fluoride and voltage in PO_4^{2-} containing electrolytes and deduced that self-organization of nanotubes was lost at higher potentials and required post annealing for crystallization. In earlier work of V. Zwilling et al. [9,10], an attempt to grow self-organized TiO_2 nanotubes in chromic oxide and hydrofluoric acid showed wide variation in tube wall thickness. It was due to current fluctuations by non-steady state conditions in the dissolution and growth of TiO_2 nanotubes. The effect of pH, conductivity of electrolyte, cyclic potential ramp to produce high aspect ratio TiO_2 nanotubes was also investigated. The formation of hexagonal

* Corresponding author. Tel.: +1 956 665 3691; fax: +1 956 665 3527.
E-mail address: haiderw@utpa.edu (W. Haider).

0013-4686/$ – see front matter © 2013 Elsevier Ltd. All rights reserved.
http://dx.doi.org/10.1016/j.electacta.2013.11.108

Table 1
Chemical composition of different electrolytes used for anodization.

Chemical	AN-1	AN-2	AN-3	AN-4	AN-5
NH_4Cl	-	1 M	-	-	-
H_2SO_4	30%	-	-	-	-
NH_4F	-	-	0.05 M	0.10 M	0.15 M
$NH_4H_2PO_4$	-	-	0.5 M	0.5 M	0.5 M
Ethylene Glycol	-	10 ml	0.1 ml	0.1 ml	0.1 ml
Glycerol	-	-	0.1 ml	0.1 ml	0.1 ml
Water	Bal.	Bal.	Bal.	Bal.	Bal.
Voltage	45V	45V	45V	45V	45V
Time (Min)	120	120	120	120	120

structure in ethylene glycol solutions was done by S. P. Albu et al. [11].

The optimization of anodizing conditions is essential to achieve specific objectives such as photocatalysis. The inherent empty $3d^2$ in Ti defines the conduction band edge and $2p^2$ state in oxygen form the valence state in TiO_2 which result in the formation of 3.2 and 3.0 eV band gap in anatase and rutile, respectively [12,13]. The additional energy levels within the band gap of anatase and rutile are generated by distorted structure TiO_2 and make them attractive member for number of electrical and optical applications. To avoid hindrance in photo-conductivity from TiO_2 nanotubes walls and eliminating sub bands to decrease the possibilities of recombination of charges post annealing is done to enhance crystallinity of as synthesized TiO_2.

The surface conditions, nature of electrolyte, concentration of fluoride ions, voltage ramp and ultimate potential are of great concern. The importance of TiO_2 nanotubes in many applications and evaluation of TiO_2 nanotubes formation mechanism were the motivation for this study. In this regard, to understand the mechanism of formation and growth of TiO_2 nanotubes during electrochemical anodizing process, various electrolytes with and without halide ions were used. The electrochemical methods such as potentiodynamic anodic polarization and electrochemical impedance spectroscopy were employed to investigate the nanotubes formation. Furthermore, the morphology of the surface after anodization process as a function fluoride ions concentration was correlated quantitatively with equivalent electrical models.

2. Experimental

The analytical grade chemicals i.e. ammonium fluoride (NH_4F), ammonium di-hydrogen phosphate ($NH_4H_2PO_4$), ethanol (C_2H_5OH) of BDH Analar, England; ethylene glycol ($C_2H_6O_2$) and acetone (CH_3COCH_3) of Merck; propanol-2 of BDH Prolabo, France and glycerol ($C_3H_8O_3$) of Riedel-Dehaen, France were used in this study.

Titanium alloy (Ti6Al4 V) specimens (30L X 10 W X 4 T) mm were first wire cut by EDM. All specimens were grinded successively from 180 to 2500 grit size papers followed by chemical cleaning in acetone, ethanol and deionized water (DI) respectively, before air-drying. The chemically cleaned specimens were electrochemically anodized in different solutions for 2 hours at 45 V in a two electrode cell system (graphite rod as cathode and Ti6Al4 V as anode) which is connected to a DC power supply (Matrix-MPS-300L-3). The electrolytes used in this study were 30% sulfuric acid (H_2SO_4), 1 M ammonium chloride (NH_4Cl) + 10 ml ethylene glycol and 0.5 M ammonium di-hydrogen phosphate ($NH_4H_2PO_4$) + 0.1 ml ethylene glycol + 0.1 ml glycerol + xM ammonium fluoride (NH_4F) in aqueous solutions; whereas 'xM' represents 0.05 M, 0.10 M, and 0.15 M NH_4F concentration in the separate electrolytes. The specimens anodized in these electrolytes were designated as AN-1, AN-2, AN-3, AN-4 and AN-5 respectively (Table 1). The surface features of each specimen were revealed by scanning electron microscope to validate the applied procedure for anodization. The potentiodynamic anodic polarization scans (PAPS) of specimens in these anodizing solutions were obtained to optimize applied conditions and resultant nanotubular structure. The PAPS were obtained in a three-electrode cell comprising on graphite rod (as auxiliary) and saturated calomel (as reference) electrodes. The specimens in their respective solution were polarized anodically to 6 V from open circuit potential (OCP) with a scan rate of 10 mV/sec. The electrochemical impedance spectroscopy (EIS) of specimens in anodizing solutions was also done to evaluate the electrochemical mechanism of anodic film dissolution and growth of nanotubular structure. The impedance spectra were executed by perturbing 10 mV AC potential within a frequency range 10 mHz–100 kHz in the same three electrode cell coupled with Gamry Potentiostat PC14/750.

The specimens anodized under optimized conditions were reproduced having nanotubular structure and few were heat treated in air at 350 °C (heating rate 10 °C/min) for 3 hours in muffle furnace (Wise Therm) to modify the structure. The 'as anodized' and 'heat treated' specimens are denoted by 'AN' and 'AN-HT' respectively. The crystal structures of 'AN' and 'AN-HT' specimens were investigated by x-ray diffraction (XRD, Philips and pro X-Pert software).

3. Results and Discussion

3.1. Synthesis of TiO_2 Nanotubes

The surface morphologies of specimen obtained after anodizing in different electrolytes are shown in Fig. 1. Generally, the formation of TiO_2 nanotubes is a competition of field enhanced TiO_2 growth at Ti/TiO_2 interface and field assisted dissolution of nanotubes at TiO_2/solution interface. The dominancy of either process largely depends on the electrolyte composition and process parameters [14–17].

The specimen anodized in AN-1 at 45 V was unaffected and there was no evidence of any nanotubular structure in H_2SO_4 containing aqueous media. The potentiodynamic anodic polarization curve as depicted in Fig. 2 represents the rapid increase in current upon polarizing to 1.170 V vs. OCP which is due to uniform dissolution of surface film followed by attaining a low constant current density (0.159 mA/cm^2) independent to increase in potential. This behavior was attributed to the formation of compact oxide film at the surface.

The electrochemical polishing and localized pitting of specimen surface is observed in AN-2 electrolyte that happens by overcoming of field assisted dissolution of TiO_2 barrier layer. The potential/current behavior of as prepared and pre-cleaned specimen showed a continuous increase in current density from 0.139 mA/cm^2 to 0.868 mA/cm^2 with increase in potential. The increase in current density above 3 V in PAPS was related to continuous electrochemical polishing and pitting due to the presence of Cl^- ions in the electrolyte. Changing the electrolytes composition and incorporating fluoride ions by varying NH_4F concentration (0.05 M, 0.10 M and 0.15 M) for AN-3, AN-4 and AN-5, respectively, resulted in the localized dissolution of surface and formation of localized pits. The fluoride ions in these electrolytes would produce water soluble $[TiF_6]^{2-}$ complex. Low concentration (NH_4F; 0.05 M) and high potential (45 V) produced localized dissolution and structure was comprised on pits and TiO_2 product (white color in Fig. 1). The anodic polarization scan depicted constant current density 0.569 mA/cm^2 independent to potential. This behavior was due to dissolution of barrier layer and solvation of Ti^{4+} ions in the electrolyte than formation of $[TiF_6]^{2-}$ ions complex was least progressive. On AN-4 surface, increased concentration (0.10 M, NH_4F) of fluoride ions produced almost equal tendencies of dissolution and growth of TiO_2 at Ti/TiO_2 and TiO_2/electrolyte interfaces

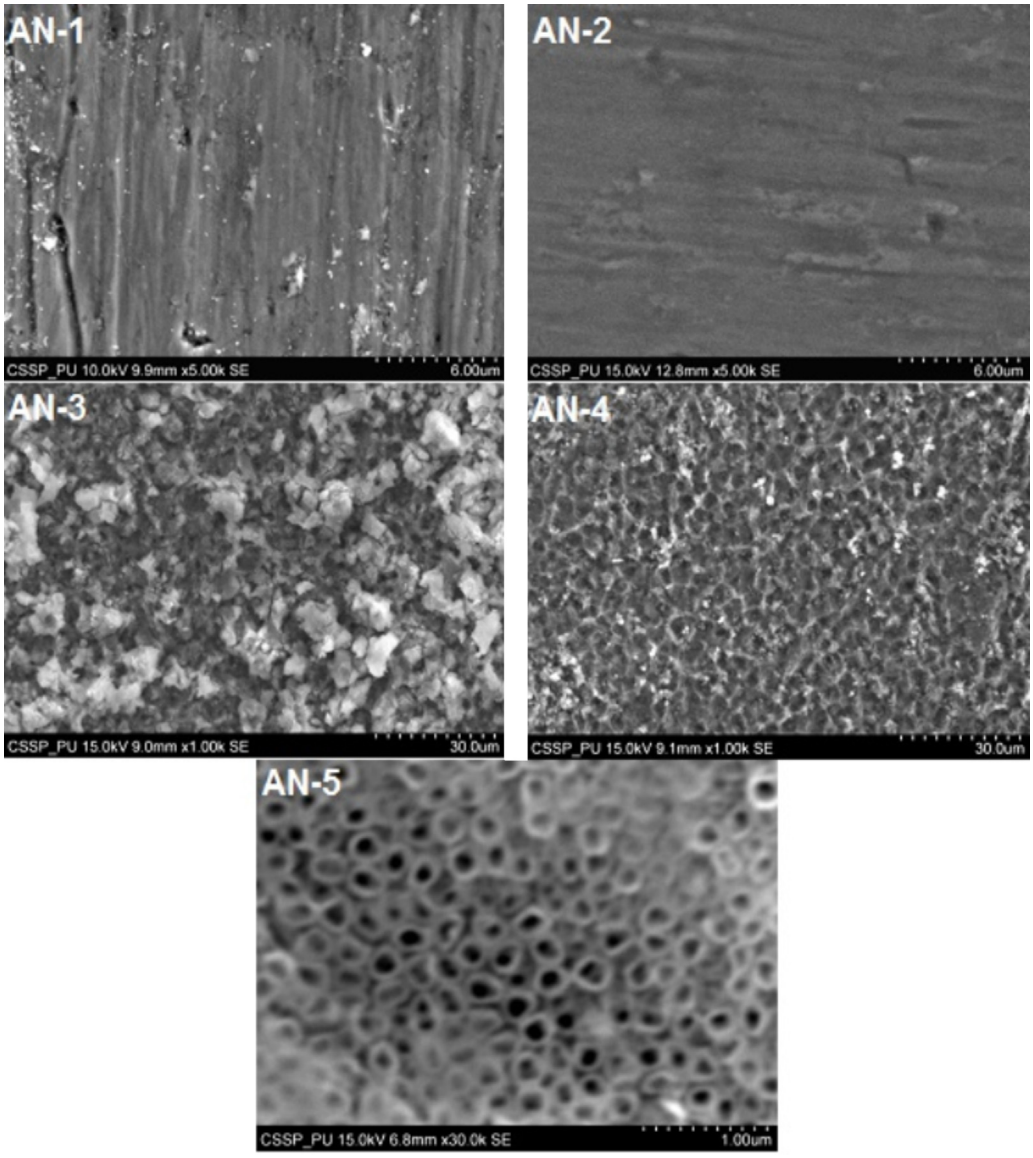

Fig. 1. Morphology of resultant surface after anodization in fluoride free (AN-1, AN-2) and fluoride containing electrolytes (AN-3, AN-4 & AN-5).

respectively. This could be evaluated from the active/passive behavior of AN-4 specimen. The initial increase in current density (5.01 mA/cm^2) was due to the formation of TiO_2 film and later drop in current density resulted in simultaneous formation of distributed pits without field assisted reaction of Ti^{4+} and OH^- ions in the electrolyte. The field assisted growth of TiO_2 nanotubes was restricted by the synergistic effect of readily available fluoride ions and higher potential. In contrast the specimen anodized in 0.15 M NH_4F solution (AN-5) the formation of nanotubular structure took place as shown in Fig. 1. The formation of TiO_2 nanotubes was observed due to sluggish field driven Ti^{4+} ions diffusion in the electrolyte (forming $[TiF_6]^{2-}$ complexes) compared to field enhanced TiO_2 growth. The formation of nanotubes at higher concentration of fluoride ions could further decrease the generation of anionic species in the electrolyte. It was confirmed in Fig. 3 that the maximum current density independent to the applied potential for anodizing was low for specimen in fluoride free electrolytes. It was further evaluated that the current density was proportional to the fluoride concentration.

3.2. Mechanism of TiO_2 Nanotubes Formation

It is well established that the formation and growth of nanotubes in fluoride containing electrolytes depends on two processes i.e., (a) field assisted oxidation of titanium at the metal/oxide interface (reactions 1 & 2) (b) field assisted chemical dissolution within the tube at TiO_2/electrolyte interface by producing water soluble complexes which controls the diameter and wall thickness of nanotubes (reactions 3 & 4) [6,18–20]. The formation and growth of nanotubes depends on the competition between mechanisms (a) and (b) as shown in Fig. 4.

$$Ti \rightarrow Ti^{4+} + 4e^- \quad (1)$$

$$Ti^{4+} + 2H_2O \rightarrow TiO_2 + 4H^+ \quad (2)$$

$$Ti^{4+} + 6F^- \rightarrow [TiF_6]^{2-} \quad (3)$$

$$TiO_2 + 6F^- + 4H^+ \rightarrow [TiF_6]^{2-} + 2H_2O \quad (4)$$

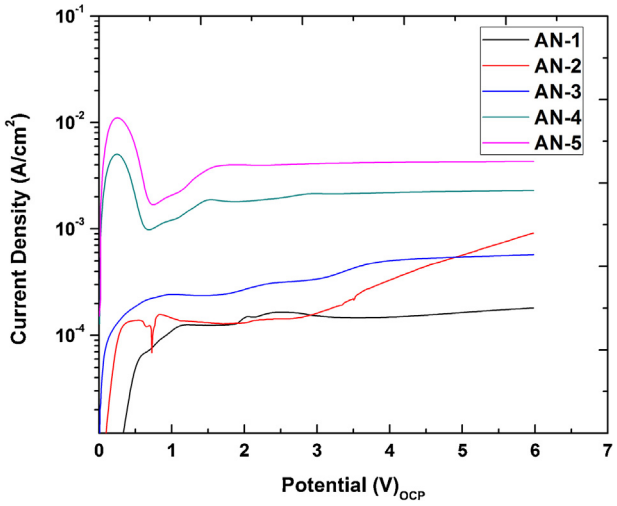

Fig. 2. Potentiodynamic Anodic Polarization scans of Ti6Al4 V alloy in various electrolytes.

The anodizing in fluoride containing AN-3 and AN-4 and at high electric field strength (45 volts), the mobility of H^+ ions towards cathode will increase and reaction 2 will proceed in forward direction with the formation of TiO_2. The presence of small fluoride ions concentration will react with Ti^{4+} (reaction 3) or will locally attack the surface by dissolving oxide film as shown in reaction 4.

Under high electric field strength and at higher concentration of F^- ions (AN-4) the field assisted oxidation at metal/electrolyte interface will be enhanced by the combined action of electrostatic charge and electrochemical attraction on H^+ ions towards cathode. The decrease in hydrogen ion concentration at the anode (Ti alloy) surface will limit the field assisted dissolution by reaction 4. This is why the white color TiO_2 product was appeared at the vicinity of pits (Fig. 1). On further increase in F^- ion concentration in AN-5 electrolyte the greater electronegativity difference between H^+ and F^- ions would suppress the approach of hydrogen ions at cathode and will be confined at the bottom of formed pit. The field assisted dissolution (reaction 4) became feasible which is responsible for tuning the shape of nanotube. Also the concentration of F^- will never drop below a critical value which is required to confine the hydrogen ions at or near bottom region of a nanotube [21]. The synergism of high field strength and high concentration of fluoride in the electrolyte will promote the growth of oxide film and

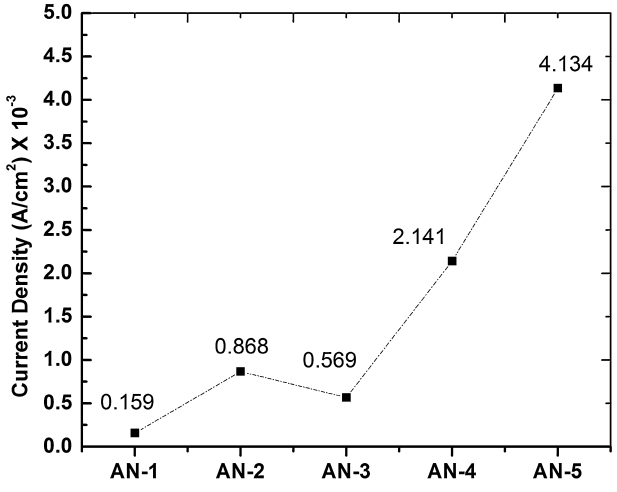

Fig. 3. Potential Independent Current density for specimens anodized in various electrolytes.

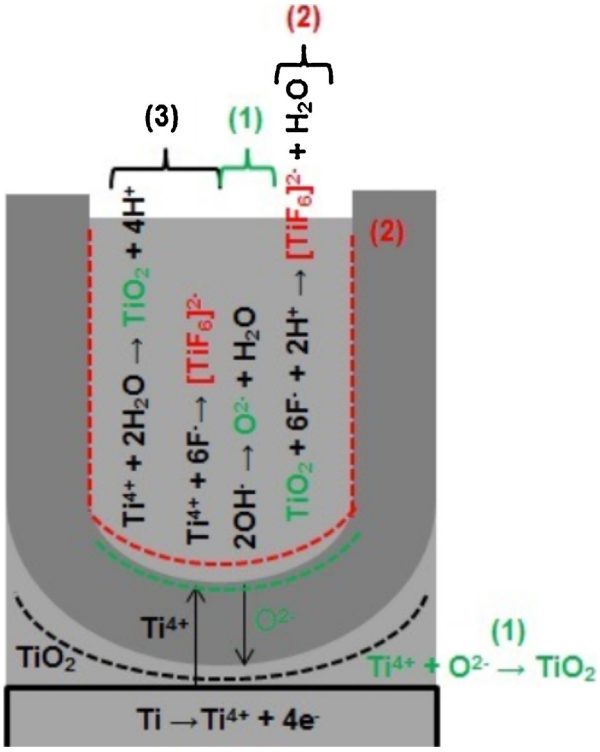

Fig. 4. Schematic mechanism of TiO_2 nanotubular structure formation in fluoride containing electrolyte (AN-5).

dissolution, respectively. The limited amount of hydrogen at the bottom of growing tube is essential for reaction 4 to proceed and controlling the diameter as well. However, increase in hydrogen ions beyond certain limit could also reverse the reaction 2. Hence, higher applied potential and relatively higher F^- ions concentration for AN-5 than AN-3 and AN-4 resulted in the formation and growth of nanotubular structure. In halide free electrolyte (AN-1) represented the formation of TiO_2 by field assisted oxidation reaction and vigorous hydrogen reduction at the surface of cathode. But with addition of NH_4Cl in the electrolyte (AN-2) there was very low restriction for hydrogen ions to move towards cathode due to relatively small electronegativity difference between Cl^- and H^+ ions. Hence, uniform field assisted dissolution was observed in combination with localized dissolution of TiO_2 at few points.

3.3. Electrochemical Impedance Spectroscopy

The EIS analysis of AN-1 and AN-2 specimens depicted single time constant due to formation of barrier type passive film and localized pitting reactions at the surface, respectively. The localized dissolution of AN-2 was correlated with the decrease in impedance (real) at low frequency as shown in Fig. 5a due to presence of chloride ions. The barrier type uniform passive film developed on AN-1 surface as estimated by the high 'R_{ct}' (17.23 kΩ-cm^2) value. The R_{ct} value for AN-2 was relatively low (1.331 kΩ-cm^2) and resistance to absorb O^{2-} (oxygenase ion) to form uniform passive film was 1.574 kΩ-cm^2. The experimental values calculated from EIS spectra by EChem Analyst software were fitted in equivalent electrical models as given in Table 2. The smallest value of goodness of fit suggested the lowest residual errors in the experimental data after fitting to equivalent electrical models.

Fig. 5b shows the nyquist plots for AN-3, AN-4 and AN-5 specimens. The impedance spectra for AN-1 and AN-2 were simulated to equivalent electrical circuit model as depicted in Fig. 6a and6b respectively. In fluoride containing electrolytes two time constants

Table 2
Quantitative data of EIS measurements and simulated with an equivalent electrical circuits.

Sample ID	R_s(Ω-cm^2)	R_{ct}(Ω-cm^2)	$(CPE)_{ct}$(μS.s$^n{}_1$/cm^2)	n_1	R_{ad}(Ω-cm^2)	$(CPE)_{ad}$(mS.s$^n{}_2$/cm^2)	n_2	L(μH/cm^2)	Goodness of Fit
AN-1	10.22	17230	161.0	0.94	-	-	-	-	0.0024
AN-2	5.224	1331	149.9	0.91	1574.0	0.000017	0.141	-	0.024
AN-3	7.962	50.12	404.9	0.47	-11.70	-455.7	0.018	23.35	0.0023
AN-4	1.672	20.42	179.7	0.77	15.66	18.02	0.160	1.309	0.0071
AN-5	4.025	14.41	171.0	0.49	9.177	23.86	0.125	0.736	0.0020

were modeled to electrical circuit as shown in Fig. 6c. The first time constant was related to charge transfer by field assisted electrochemical reactions of Ti^{4+} and TiO_2 by fluoride ions at TiO_2/electrolyte interface and second constant was corresponded to adsorption of O^{2-} ions at Ti/TiO_2 interface by following reactions 5 and 6, respectively.

$$Ti^{4+} + 2H_2O + 6F^- \rightarrow [TiF_6]^{2-} + 4H^+ + 2O^{2-} \quad (5)$$

$$Ti^{4+} + 2O^{2-} \rightarrow TiO_2 \quad (6)$$

However, the small concentration of fluorides facilitated the local pitting but was not enough to aid electrochemical oxidation and simultaneous reduction of water to produce O^{2-} ions [22]. The inductive behavior at low frequency was also observed in impedance spectrum due to successive charge transfer reaction and adsorption of O^{2-} ions to form TiO_2 at metal/oxide interface [23].

The dispersion of ideal capacitance to constant phase element (CPE) was due to surface roughness and heterogeneous adsorption of anions at the surface. It was clear that increasing the fluoride concentration in the electrolyte decreased the charge transfer resistance (R_{ct}). The CPE values at the distorted double layer also decreased from 404.9 to 179.7 and further reached to 171.0 μS.s$^n{}_1$/cm^2 by spontaneous charge dissipation in combination with adsorption of O^{2-} anions hence resulted in growth of TiO_2 porous structure in AN-5 electrolyte. The pseudoresistive and pseudocapacitive (negative values of R_{ad} and $(CPE)_{ad}$) for AN-3 specimen suggested the deficiency of O^{2-} and ultimately uniform pitting was observed by fluoride ions as shown in Fig. 1. In other words, the negative values of R_{ad} and $(CPE)_{ad}$ attributed to the higher desorption tendency of O^{2-} resulting in pitting and formation of oxide product. The localized dissolution was accelerated by potential dependent faradaic electron transfer by fluoride ions and change in oxidation state from Ti^{4+} to water soluble $[TiF_6]^{2-}$. The high inductance value at low frequency regime corresponded to the accelerated oxidation of Ti to Ti^{4+} followed by formation of water soluble $[TiF_6]^{2-}$. The resistance to adsorb O^{2-} ions at the surface and limited capacity for adsorption under applied potential was estimated from quantitative data for AN-4. The decrease in R_{ct} with increase in fluoride ions

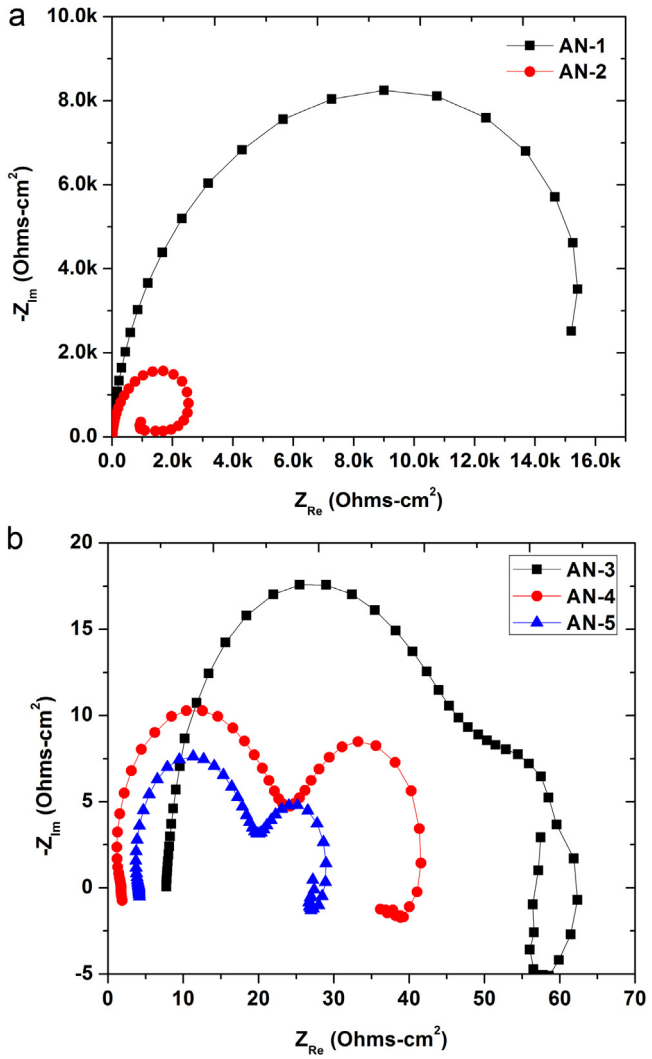

Fig. 5. Electrochemical Impedance Spectrums (a) Fluoride free electrolytes (AN-1, AN-2) (b) Fluoride containing electrolytes (AN-3, AN-4 & AN-5).

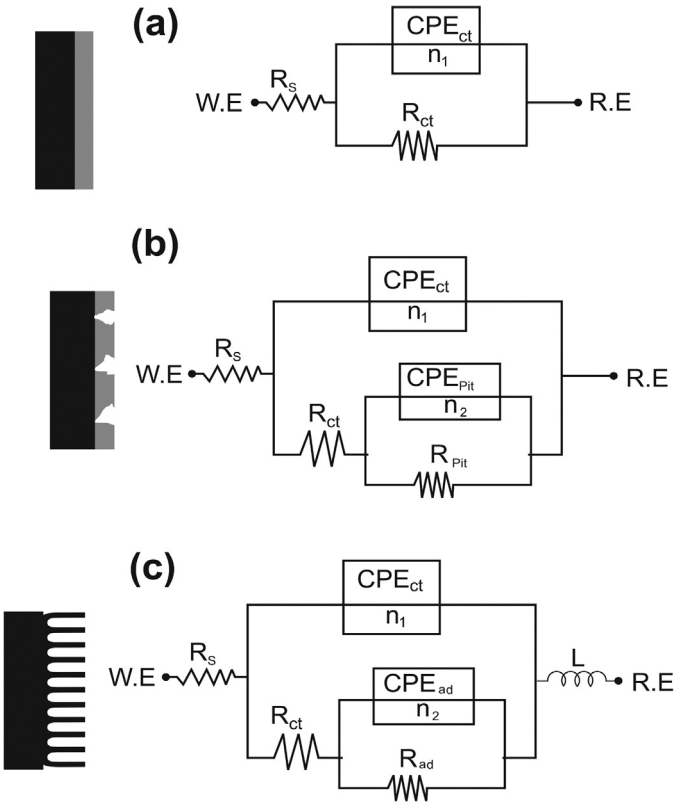

Fig. 6. Simulated equivalent electrical circuit models for EIS spectrums in different electrolytes.

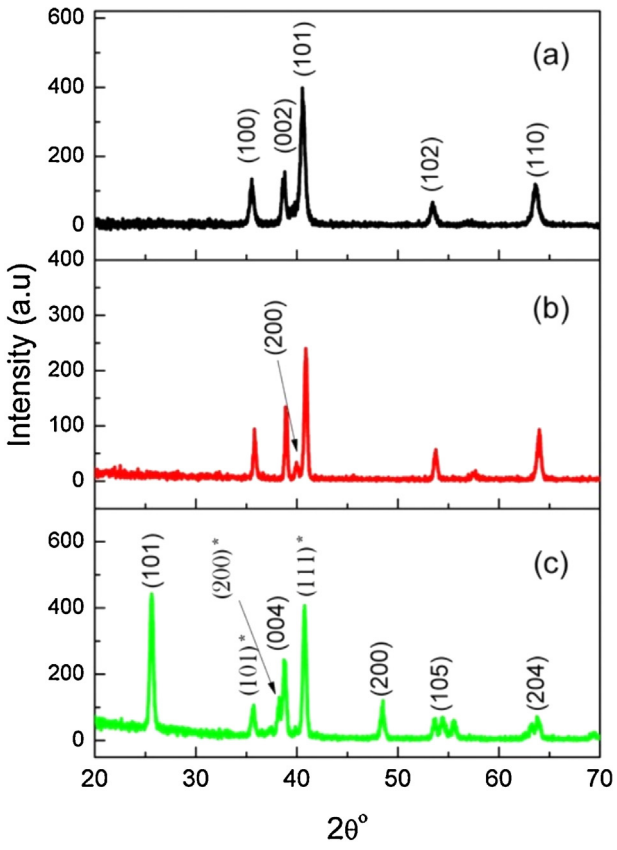

Fig. 7. XRD patterns of (a) Untreated (b) As Anodized (AN) (c) Anodized and Heat Treated.

concentration would have least influence on adsorption of oxygen ions at the surface than forming water soluble complex structure species. These results also suggests that higher concentration of F^- ions (AN-5) at the tube mouth would have more electrostatic attraction towards hydrogen ions (H^+) (generated at the tube bottom during field assisted oxidation) in addition with applied field strength on fluoride ions toward tube bottom (for field assisted dissolution of TiO_2).The relatively lower R_{ad} and higher $(CPE)_{ad}$ for AN-5 than AN-4 specimen was due to dominancy of field assisted TiO_2 growth by reaction of Ti^{4+} with O^{2-} over field assisted dissolution by fluoride ions. The decrease in low frequency inductance was in support to the formation of TiO_2 with limited tendency of charge dissipation or higher adsorption of O^{2-} ions. The slight increase in the solution resistance for AN-5 specimen electrolyte was due to actual increase in average electrolyte thickness form tube bottom to the luggin capillary of reference electrode.

4. X-Ray Diffraction of As Anodized (AN) and Heat Treated (AN-HT) Specimens

In Fig. 7a, all the peaks were the characteristic peaks of titanium as they were exactly matching with titanium reference pattern in ICSD PDF-2 database release 2007 (# 01-001-1198). The XRD pattern of anodized sample (Fig. 7b), showed similar peaks as that of 'Ti', however, their intensity has decreased slightly while a new peak (200) at 40.58° appeared which was due to Ti_6O as it is matching to reference pattern of Ti_6O (01-072-1807). The drop in intensity of anodized sample and absence of typical titanium dioxide peaks showed that the anodized film is very thin and lacks oxygen for the development of proper rutile or anatase phases. The XRD pattern of as anodized (AN) and heat-treated sample (AN-HT) clearly confirmed that the heat treatment in air; aided the formation of more oxidized and regular phases. The spectrum in Fig. 7c showed that many peaks (without asterisk superscript) were the characteristics of anatase phase (01-076-0326), whereas few peaks, labeled with asterisk, were due to rutile phase (01-076-0326). It is clear from the XRD analysis that heat treatment of anodized titanium favors the formation of anatase with very low content of rutile phase.

5. Conclusion

It is concluded that the surface features of Ti6Al4 V alloy after anodizing largely depends on the electrolyte composition. The formation of compact oxide film was evident in halide free (H_2SO_4) electrolyte which was in support to constant but low current density value in PAPS analysis and development of large R_{ct} in single time constant impedance spectrum. The relatively higher current density and appearance of inductive behavior at low frequency regime of nyquist plot supported the simultaneous electropolishing and pitting of specimens in chloride containing electrolyte, respectively. Different surface morphologies in fluoride containing electrolytes at similar process parameters validated the dominancy of either field enhanced TiO_2 nanotubes growth or field assisted dissolution of Ti/TiO_2. It was also confirmed that at low F^- ions concentration (0.05 M NH_4F) the overcoming of field assisted dissolution resulted in the distributed pits without field assisted reaction of Ti^{4+} and OH^- hence limited TiO_2 growth. The negative values of 'R_{ad}' and $(CPE)_{ad}$ were in support to the high desorption tendency of oxygenase ions. The decrease in R_{ct} and R_{ad} and increase in charge capacity (higher $(CPE)_{ad}$) due to O^{2-} ions adsorption on increasing F^- ions in electrolyte resulted in the formation of nanotubular structure. X-ray diffraction patterns suggested the formation of oxygen deficient Ti_6O phase which corresponded to distorted structure of rutile. The heat treatment of as anodized specimen (AN-5) in air transformed Ti_6O to rutile and anatase phases.

Acknowledgement

W. Haider would like to acknowledge 2013 Ralph E. Powe Junior Faculty Enhancement Award.

References

[1] Williams, D. F., Titanium and titanium alloys, in 'Biocompatibility of Clinical Implant Materials', Vol. I, CRC, Press, Boca Raton, FL, USA, 1981.
[2] B. Bozinni, P. Carlino, L. D'Urzo, V. Pepe, C. Mele, F. Venturo, An electrochemical impedance investigation of the behavior of anodically oxidized titanium in human plasma and cognate fluids, relavant to dental applications, J. Mater. Sci: Mater. Med. 19 (2008) 3443.
[3] J.C. Marchenoir, J.P. Loup, J. Masson, Étude des couches poreuses formées par oxydation anodique du titane sous fortes tensions, Thin Solid Films 66 (3) (1980) 357.
[4] J.W. Schultze, M.M. Lohrengel, Nucleation and growth of anodic oxide films, Electrochimi. Acta 28 (7) (1983) 973.
[5] K.S. Brammer, S. Oh, C.J. Cobb, L.M. Bjursten, H.V.D. Heyde, S. Jin, Improved bone-forming functionality on diameter-controlled TiO_2 nanotube surface, Acta Biomaterialia 5 (8) (2009) 3215.
[6] D. Gong, C.A. Grimes, O.K. Varghese, W. Hu, R.S. Singh, Z. Chen, E.C. Dickey, Titanium oxide nanotube arrays prepared by anodic oxidation, J. Mater. Res. 16 (12) (2001) 3331.
[7] A. Ghicov, H. Tsuchiya, J.M. Macak, P. Schmuki, Titanium oxide nanotubes prepared in phosphate electrolytes, Electrochem. Commun. 7 (5) (2005) 505.
[8] S. Bauer, S. Kleber, P. Schmuki, TiO_2 nanotubes: Tailoring the geometry in H_3PO_4/HF electrolytes, Electrochem. Commun. 8 (8) (2006) 1321.
[9] V. Zwilling, E. Darque-Ceretti, A. Boutry-Forveille, D. David, M.Y. Perrin, M. Aucouturier, Structure and physicochemistry of anodic oxide films on titanium and TA6 V alloy, Surf. Interface Anal. 27 (7) (1999) 629.
[10] V. Zwilling, M. Aucouturier, E. Darque-Ceretti, Anodic oxidation of titanium and TA6 V alloy in chromic media: An electrochemical approach, Electrochim. Acta 45 (6) (1999) 921.
[11] S.P. Albu, A. Ghicov, J.M. Macak, P. Schmuki, 250 (m long anodic TiO_2 nanotubes with hexagonal self-ordering, Physica. Status Solidi. (RRL) 1 (2) (2007) R65.
[12] R. Asahi, Y. Taga, W. Mannstadt, A.J. Freeman, Electronic and optical properties of anatase TiO_2, Phys. Rev. B 61 (11) (2000) 7459.

[13] Z.Y. Wu, G. Ouvrared, P. Gressier, C.R. Natoli, Ti and O K-edges for titanium oxides by multiple scattering calculations: comparison to XAS and EELS spectra, Phys. Rev. B 55 (1997) 10382.
[14] D. Gong, C.A. Grimes, O.K. Varghese, W. Hu, R.S. Singh, Z. Chen, E.C. Dickey, Titanium oxide nanotube arrays prepared by anodic oxidation, J. Mater. Res. 16 (12) (2001) 3331.
[15] O.K. Varghese, D. Gong, M. Paulose, K.G. Ong, C.A. Grimes, E.C. Dickey, Crystallization and high-temperature structural stability of titanium oxide nanotube arrays, J. Mater. Res. 18 (1) (2003) 156.
[16] Q. Cai, M. Paulose, O.K. Varghese, C.A. Grimes, The effect of electrolyte composition on the fabrication of self-organized titanium oxide nanotube arrays by anodic oxidation, J. Mater. Res. 20 (1) (2005) 230.
[17] X. Quan, S.G. Yang, X.L. Ruan, H.M. Zhao, Preparation of titania nanotubes and their environmental applications as electrode, Environ. Sci. & Technol. 39 (10) (2005) 3770.
[18] G.K. Mor, O.K. Varghese, M. Paulose, N. Mukherjee, C.A. Grimes, Fabrication of tapered, conical-shaped titania nanotubes, J, Mater. Res. 18 (2003) 2588.
[19] M. Paulose, K. Shankar, S. Yoriya, H.E. Prakasam, O.K. Varghese, G.K. Mor, T.A. Latempa, A. Fitzgerald, C.A. Grimes, Anodic growth of highly ordered TiO_2 nanotube arrays to 134 (m in length, J. Phys. Chem. B 110 (2006) 16179–16184.
[20] K. Shankar, G.K. Mor, H.E. Prakasam, S. Yoriya, M. Paulose, O.K. Varghese, C.A. Grimes, Highly-ordered TiO_2 nanotube arrays up to 220 (m in length: use in water photoelectrolysis and dye-sensitized solar cells, Nanotechnology 18 (2007) 065707.
[21] L. Sun, S. Zhang, X.W. Sun, X. He, Effect of electric field strength on the length of anodized titania nanotube arrays, J. Electroanal. Chem. 637 (2009) 6.
[22] S.H. Kang, J.Y. Kim, H.S. Kim, Y.E. Sung, Formation and mechanistic study of self-ordered TiO_2 nanotubes on Ti substrate, J. Ind. Eng. Chem. 14 (1) (2008) 52.
[23] J.P. Diard, B. Le Gorrec, C. Montella, Calculation, simulation and interpretation of electrochemical impedences. Part 3. Conditions for observations of low frequency inductive diagrams for a two-step electron transfer reaction with an absorbed intermediate species, J. Electroanal. Chem. 326 (1992) 13.